We greatly value the careful reading and the detailed comments provided by the referees. The responses to the comments of the two referees in our direct reply (shown below) and within the revised manuscript (see marked copy) are provided below. The pages and lines indicated below correspond to those in the marked copy.

Response to Referee 1 (Referees' comments are italicized)

1. Referee comment: "*Line 278–282: What does the theory for charging effects assume about charge on the chamber walls? This can vary due to contact when conducting experiments and so may not be reproducible.*"

Author response: In the manuscript, we assume that the chamber walls are not charged. This assumption is reasonable since the FEP Teflon chamber used is housed in an enclosure (i.e., GTEC facility) to minimize contact with the chamber walls. The chamber walls were never exposed to contact in this series of experiments. Furthermore, the uncorrected particle wall-deposition coefficients for the low-SA-seed-only (experiments 1 through 4) agree with previously measured particle wall-deposition coefficients. This suggests that charging effects (if any) are reproducible as long as the chamber walls are not exposed to contact.

2. Referee comment: "*Lines 514–518: How is it known that SOA growth should stop after the α-pinene reacted? Why can't there be continued growth due to condensation driven by oligomer formation?*"

Author response: Previous studies have shown that even though α-pinene ozonolysis forms oligomers from particle phase reactions, SOA growth still essentially stops once all the α-pinene has reacted (Gao et al., 2004a and 2004b; Ng et al., 2006). These references have been added to the revised manuscript:

Page 13 line 378: "SOA growth basically ceases once all the α-pinene has reacted, indicating that the first step of α-pinene ozonolysis is rate-limiting and the first-generation products are condensable (Gao et al., 2004a and 2004b; Ng et al., 2006; Chan et al., 2007)."

Page 13 line 386: "In cases where the coagulation-corrected size-dependent particle wall-deposition coefficients are used to correct for particle wall-deposition (Figs. 3a-d), the SOA growth profile is similar to that of the low-SA experiments; SOA growth essentially stops once all the α-pinene has reacted, as expected (Gao et al., 2004a and 2004b; Ng et al. 2006; Chan et al., 2007)."

References:

Chan, A. W. H., Kroll, J. H., Ng, N. L., and Seinfeld, J. H.: Kinetic modeling of secondary organic aerosol formation: effects of particle- and gas-phase reactions of semivolatile products, Atmospheric Chemistry and Physics, 7, 4135-4147, 2007.

Gao, S., Ng, N. L., Keywood, M., Varutbangkul, V., Bahreini, R., Nenes, A., He, J. W., Yoo, K. Y., Beauchamp, J. L., Hodyss, R. P., Flagan, R. C., and Seinfeld, J. H.: Particle phase acidity and oligomer formation in secondary organic aerosol, Environmental Science & Technology, 38, 6582-6589, 10.1021/es049125k, 2004a.

Gao, S., Keywood, M., Ng, N. L., Surratt, J., Varutbangkul, V., Bahreini, R., Flagan, R. C., and Seinfeld, J. H.: Low-molecular-weight and oligomeric components in secondary organic aerosol from the ozonolysis of cycloalkenes and alpha-pinene, J. Phys. Chem. A, 108, 10147-10164, 10.1021/jp047466e, 2004b.

Ng, N. L., Kroll, J. H., Keywood, M. D., Bahreini, R., Varutbangkul, V., Flagan, R. C., Seinfeld, J. H., Lee, A., and Goldstein, A. H.: Contribution of first- versus second-generation products to secondary organic aerosols formed in the oxidation of biogenic hydrocarbons, Environmental Science & Technology, 40, 2283-2297, 10.1021/es052269u, 2006.

3. Referee comment: "*Lines 514–518: How can all three methods be effective for correcting for wall loss when they give such different results?*"

Author response: In our experiments that use low seed aerosol surface area concentrations (< 3000 μm^2 cm^{-3}), SOA mass yields at peak SOA growth obtained from the "size-dependent", "number averaged" and "volume averaged" methods agree within 14% (Figs. 5 and 6). Hence, our results indicate that these three methods are effective in correcting for particle wall loss in experiments that use low seed aerosol surface area concentrations.

In our experiments that use high seed aerosol surface area concentrations (≥ 8000 μm^2 cm^{-3}), SOA mass yields at peak SOA growth obtained from the "size-dependent", "number averaged" and "volume averaged" methods differ substantially (Figs. 5 and 6). As explained in the manuscript, these differences arise from assumptions made in the particle wall-deposition correction method regarding the influence of coagulation on the first-order particle wall-loss rate. We find that coagulation needs to be accounted for when the "size-dependent" and "number averaged" particle wall-deposition correction methods are used in chamber studies that utilize high seed aerosol surface area concentrations.

To remove any confusion regarding the effectiveness of the "size-dependent", "number averaged" and "volume averaged" methods in correcting for particle wall deposition at different seed aerosol surface area concentrations, the following changes have been made to the revised manuscript:

Page 19 line 567: "In the experiments with low seed aerosol surface area concentrations (< 3000 μm^2 cm^{-3}), the SOA mass yields obtained by the different particle wall-deposition correction methods (i.e., the "size-dependent", "number averaged" and "volume averaged" methods) are generally consistent with one another. This indicates that these three methods are effective in correcting for particle wall-deposition in experiments that use low seed aerosol surface area concentrations. However, in the experiments with high seed aerosol surface area concentrations (≥ 8000 μm^2 cm^{-3}), the calculated SOA mass yields differ substantially. These differences arise from assumptions made in the particle wall-deposition correction method regarding the influence of coagulation on the first-order particle wall-loss rate. Specifically, we find that coagulation needs to be accounted for in the "size-dependent" and "number averaged" methods in order for them to be effective in chamber studies that use high seed aerosol surface area concentrations. Coagulation does not need to be accounted for in the "volume averaged" method since coagulation does not affect aerosol volume concentrations."

4. Referee comment: "*Lines 584–593: Similar to Comment 3. The recommendations are a bit*

unclear, considering that the methods can give significantly different corrections."

Author response: Please refer to our response to comment 3. In addition, the original manuscript provides explicit recommendations regarding the use of different particle wall-deposition methods in chamber studies (regardless of VOC system) that use high seed aerosol surface area concentrations:

Page 20 line 591: "Here we showed that the condensation of SOA-forming vapors in the α-pinene ozonolysis system can be erroneously concluded as kinetically limited if coagulation is not accounted for in the "size-dependent" and "number averaged" particle wall-deposition correction methods. Similar flawed conclusions in other VOC systems may be drawn in chamber studies that use high seed aerosol surface area concentrations to promote SOA formation but do not account for coagulation. Therefore, we recommend accounting for coagulation when the "size-dependent" and "number averaged" particle wall-deposition correction methods are used in chamber studies that use high seed aerosol surface area concentrations (e.g., ≥ 3000 μm^2 cm^{-3}) to promote the condensation of SOA-forming vapors onto seed aerosol regardless of VOC system. Alternatively, the "volume averaged" and "inert tracer" methods can be used in chamber studies that use high seed aerosol surface area concentrations. In addition, we suggest using multiple techniques (i.e., at least 2) to correct for particle wall-loss in order to determine the effect of SOA mass yield uncertainties introduced by particle wall-deposition correction."

5. Referee comment: "*Conclusions. It would be worth noting that it is also possible to use a slightly different inert tracer method that does not assume that the particles on the wall remain in equilibrium with suspended particles. One can use the decay of the AMS seed signal after peak SOA to estimate a wall-loss rate coefficient and then apply this to the rest of the experiment. It is similar then to the volume average method, except that the measured wall-loss rate coefficient is not affected by changes in particle volume due to evaporation after peak SOA is reached. Measuring time-profiles of different AMS masses relative to the seed also gives information on whether the particle composition is changing due to condensation or evaporation.*"

Author response: One of the main objectives of this manuscript to evaluate the effectiveness of commonly used particle wall-deposition correction methods. While the referee is correct that the decay of the seed aerosol signal measured by an aerosol mass spectrometer can be used to estimate a first-order particle wall-deposition rate, this particle wall-deposition correction method is not commonly used. Hence, we did not include this suggestion in the revised manuscript.

6. Referee comment: "*In this analysis it is assumed that the results are unaffected by vapor loss to the walls. Are there situations where particle and vapor wall loss are closely coupled, and so cannot be interpreted as separate processes as was done here?*"

Author response: We did not assume that our results are unaffected by vapor wall deposition in our analysis. Instead, we showed explicitly in a previous paper that SOA formation in the α-pinene ozonolysis system is governed by quasi-equilibrium growth (i.e., the timescale for gas-particle equilibrium is less than those for reaction and vapor wall-loss), which results in SOA growth being independent of the seed aerosol surface area concentration (Nah et al., 2016). To remove any confusion, the following changes have been made to the revised manuscript:

Page 5 line 142: "This work builds on our previous study on the influence of seed aerosol surface area concentration and hydrocarbon oxidation rate on vapor wall deposition and SOA mass yields in the α-pinene ozonolysis system (Nah et al., 2016). In our previous study, we used a coupled vapor-particle dynamics model to show that the condensation of SOA-forming vapors onto seed aerosol in the α-pinene ozonolysis system is dominated by quasi-equilibrium growth. This present work is aimed at understanding the uncertainties in the SOA mass yields due to the application of different particle wall-deposition correction methods."

Reference:

Nah, T., McVay, R. C., Zhang, X., Boyd, C. M., Seinfeld, J. H., and Ng, N. L.: Influence of seed aerosol surface area and oxidation rate on vapor wall deposition and SOA mass yields: a case study with α-pinene ozonolysis, Atmos. Chem. Phys., 16, 9361-9379, 10.5194/acp-16-9361-2016, 2016.

It is possible that particle and vapor wall deposition processes may be closely coupled in VOC systems where the condensation of SOA-forming vapors onto seed aerosol is kinetically limited (i.e., the timescale for gas-particle equilibrium is competitive with or greater than those for reaction and vapor wall-loss). In these systems, large concentrations of seed aerosol can be added to promote gas-particle partitioning, and consequently increase SOA mass yields. Hence, it is possible that faster particle wall deposition rates may result in a larger effect of vapor wall deposition on SOA formation (and vice versa) in systems where SOA formation is governed by kinetically limited growth.

7. Referee comment: "*It would also be useful to provide some comments on at least one approach that could be used to avoid complications from wall loss of particles and vapor, which is to conduct short experiments.*"

Author response: We thank the referee for this suggestion. This is included in the revised manuscript:

Page 20 line 605: "Complications arising from particle and vapor wall deposition may also be potentially minimized by conducting shorter chamber experiments. This can be achieved by using excess oxidant concentrations, which will increase the oxidation rate, and consequently reduce the time at which peak SOA growth is achieved (Nah et al., 2016)."

8. Referee comment: "*Technical Comments. Throughout the paper the authors jump between the term "volume averaged" and "volume dependent" method. I suggest sticking with one or the other.*"

Author response: In the revised manuscript, we use the term "volume averaged".

Response to Referee 2 (Referees' comments are italicized)

We thank the referee for the positive comments.

1 **Constraining uncertainties in particle wall-deposition correction during SOA**
2 **formation in chamber experiments**

4 T. Nah,[1] R. C. McVay,[2] J.R. Pierce,[3] J. H. Seinfeld[2,4] and N. L. Ng[1,5*]
5
6 [1]*School of Chemical and Biomolecular Engineering, Georgia Institute of Technology, Atlanta, GA, USA*
7 [2]*Division of Chemistry and Chemical Engineering, California Institute of Technology, Pasadena, CA, USA*
8 [3]*Depratment of Atmospheric Science, Colorado State University, Fort Collins, CO, USA*
9 [4]*Division of Engineering and Applied Science, California Institute of Technology, Pasadena, CA, USA*
10 [5]*School of Earth and Atmospheric Sciences, Georgia Institute of Technology, Atlanta, GA, USA*
11
12 ** To whom correspondence should be addressed: ng@chbe.gatech.edu*

14 **Abstract**

15 The effect of vapor wall-deposition on secondary organic aerosol (SOA) formation has

16 gained significant attention; however, uncertainties in experimentally derived SOA mass

17 yields due to uncertainties in particle wall-deposition remain. Different approaches have

18 been used to correct for particle wall-deposition in SOA-formation studies, each having

19 its own set of assumptions in determining the particle wall-loss rate. In volatile and

20 intermediate-volatility organic compound systems in which SOA formation is governed

21 by kinetically limited growth, the effect of vapor wall-deposition on SOA mass yields can

22 be constrained by using high surface area concentrations of seed aerosol to promote the

23 condensation of SOA-forming vapors onto seed aerosol instead of the chamber walls.

24 However, under such high seed aerosol levels, the presence of significant coagulation

25 may complicate the particle wall-deposition correction. Here, we present a model

26 framework that accounts for coagulation in chamber studies in which high seed aerosol

27 surface area concentrations are used. For the α-pinene ozonolysis system, we find that,

28 after accounting for coagulation, SOA mass yields remain approximately constant when

29 large seed aerosol surface area concentrations ($\geq$ 8000 μm^2 cm^{-3}) are used, consistent

30 with our prior study (Nah et al., 2016) that α-pinene ozonolysis SOA formation is

31 governed by quasi-equilibrium growth. In addition, we systematically assess the

32 uncertainties in the calculated SOA mass concentrations and yields between four

33 different particle wall-loss correction methods over the series of α-pinene ozonolysis

34 experiments. At low seed aerosol surface area concentrations (< 3000 μm^2 cm^{-3}), the

35 SOA mass yields at peak SOA growth obtained from the particle wall-loss correction

36 methods agree within 14 %. However, at high seed aerosol surface area concentrations ($\geq$

37 8000 μm^2 cm^{-3}), the SOA mass yields at peak SOA growth obtained from different

38 particle wall-loss correction methods can differ by as much as 58 %. These differences

39 arise from assumptions made in the particle wall-loss correction regarding the first-order

40 particle wall-loss rate. This study highlights the importance of accounting for particle

41 wall-deposition accurately during SOA-formation chamber experiments and assessing the

42 uncertainties associated with the application of the particle wall-deposition correction

43 method when comparing and using SOA mass yields measured in different studies.

44 **1. Introduction**

45   Secondary organic aerosol (SOA), which constitutes a large mass fraction of fine

46 atmospheric particulate matter, is formed from the oxidation of volatile and intermediate-

47 volatility organic compounds (VOCs and IVOCs) followed by gas-particle partitioning

48 (Kanakidou et al., 2005; Kroll and Seinfeld, 2008; Hallquist et al., 2009; Tsigaridis et al.,

49 2014). Laboratory chambers are typically used to study SOA formation from VOC and

50 IVOC oxidation in a controlled environment. SOA mass yields (Y), defined as the ratio

51 of mass concentration of SOA formed (ΔM_o) to the mass concentration of reacted

52 hydrocarbon (ΔHC) (Y = $\Delta M_o/\Delta HC$), are measured in these chamber experiments (Odum

53 et al., 1996; Odum et al., 1997a; Odum et al., 1997b). Interpretation of data derived from

54 such experiments is complicated by the fact that particles and SOA-forming vapors

55 deposit on the chamber walls throughout an experiment (Crump and Seinfeld, 1981;

56 McMurry and Grosjean, 1985; McMurry and Rader, 1985; Cocker et al., 2001; Weitkamp

57 et al., 2007; Pierce et al., 2008; Hildebrandt et al., 2009; Loza et al., 2010; Matsunaga and

58 Ziemann, 2010; Loza et al., 2012; Kokkola et al., 2014; McVay et al., 2014; Yeh and

59 Ziemann, 2014; Zhang et al., 2014; Yeh and Ziemann, 2015; Zhang et al., 2015;

60 Krechmer et al., 2016; La et al., 2016; McVay et al., 2016; Ye et al., 2016; Nah et al.,

61 2016). Failure to account for particle and vapor wall-losses accurately will result in

62 incorrect SOA mass yields, which will lead to flawed predictions of ambient SOA mass

63 concentrations (Cappa et al., 2016).

64   Particles deposit on the chamber walls via diffusion, gravitational settling and

65 electrostatic forces (Crump and Seinfeld, 1981; McMurry and Grosjean, 1985; McMurry

66   and Rader, 1985; Pierce et al., 2008). The rate at which particles deposit on chamber

67   walls depends on particle size. The particle wall-loss mechanism for uncharged particles

68   in an uncharged chamber is similar to that of the dry deposition of particles (Pierce et al.,

69   2008; Seinfeld and Pandis, 2016). Small particles are transported by Brownian diffusion

70   through the boundary layer adjacent to the chamber walls, while the loss of large particles

71   is governed by gravitational settling. Particle wall-loss rates are enhanced if the particles

72   and/or chamber walls are charged (McMurry and Grosjean, 1985; McMurry and Rader,

73   1985; Pierce et al., 2008). Smaller charged particles deposit more efficiently than larger

74   charged particles due to their larger Brownian diffusion rates and charge-to-mass ratios.

75   Several methods have been used to account for particle wall-deposition in SOA-

76   formation studies. In one particle wall-loss correction method, the rate of decay of

77   polydisperse inert seed aerosol (e.g., ammonium sulfate particles) is measured in periodic

78   seed-only experiments (Keywood et al., 2004; Pierce et al., 2008). Size-dependent

79   particle wall-deposition coefficients are then obtained by fitting a first-order exponential

80   decay to the measured particle number concentration decay in each size bin. The total

81   aerosol number concentration usually needs to be sufficiently low in these seed-only

82   experiments such that the effect of coagulation is negligible. In cases in which high seed

83   aerosol number concentrations are used, an aerosol dynamics model can be applied to

84   correct the particle wall-deposition coefficients for coagulation. Particle wall-loss in a

85   SOA formation experiment is then accounted for using these size-dependent particle

86   wall-deposition coefficients to obtain the total SOA mass concentration. A key

87   assumption of this approach is that the size-dependent particle wall-deposition

88   coefficients do not change between these seed-only and SOA-formation experiments.

89   Other previously reported particle wall-loss correction methods do not require the use of

90   separate seed-only experiments to characterize particle wall-loss rates. Instead, the

91   average loss rate of the total aerosol mass or number concentration is measured directly

92   during the SOA formation experiment (Carter et al., 2005; Pathak et al., 2007; Pierce et

93   al., 2008; Hildebrandt et al., 2009). The measured average particle loss rate is then

94   applied to the entire experiment to correct for particle wall-deposition. A key assumption

95   of this approach is that the particle wall-loss rate is not strongly dependent on particle

96   size, thus allowing for the overall particle wall-loss to be characterized by a single decay

97 rate coefficient. The extent to which these methods account for particle wall-deposition in

98 SOA-formation studies performed in a chamber, in which particle wall-loss rates are

99 known to strongly depend on particle size, is unclear. Therefore, SOA mass yield

100 uncertainties associated with the application of different particle wall-loss correction

101 methods need to be evaluated when comparing and using SOA mass yields measured in

102 different studies. This is the subject of the present work.

103   Previous studies have shown that SOA mass yields can be substantially

104 underestimated if the loss of SOA-forming vapors to chamber walls is not accounted for

105 (Matsunaga and Ziemann, 2010; McVay et al., 2014; Yeh and Ziemann, 2014; Zhang et

106 al., 2014; Yeh and Ziemann, 2015; Zhang et al., 2015; Krechmer et al., 2016; La et al.,

107 2016; McVay et al., 2016; Ye et al., 2016; Nah et al., 2016). Unlike particle wall-loss,

108 experimental methods for estimating vapor wall-loss rates in chambers are not yet well

109 established. However, the extent to which vapor wall-loss impacts SOA mass yields can

110 be characterized and quantified using time-dependent, parameterizable models that use

111 the measured SOA mass concentrations as model inputs (Zhang et al., 2014). Recent

112 studies have shown that the addition of large concentrations of seed aerosol can promote

113 gas-particle partitioning, and consequently increase SOA mass yields in VOC systems

114 where the condensation of SOA-forming vapors onto seed aerosol is kinetically limited

115 (i.e., the timescale for gas-particle equilibrium is competitive with or greater than those

116 for reaction and vapor wall-loss) (Riipinen et al., 2011; Zhang et al., 2012; McVay et al.,

117 2014; Zhang et al., 2014). In contrast, SOA growth is independent of seed aerosol surface

118 area in VOC systems in which the condensation of SOA-forming vapors onto seed

119 aerosol is governed by quasi-equilibrium growth (i.e., the timescale for gas-particle

120 equilibrium is less than those for reaction and vapor wall-loss) (Riipinen et al., 2011;

121 Zhang et al., 2012; McVay et al., 2014; McVay et al., 2016; Nah et al., 2016). Together,

122 these studies show that the role of gas-particle partitioning (i.e., kinetically limited vs.

123 quasi-equilibrium SOA growth) in influencing vapor wall-deposition can be inferred

124 from the relationship between SOA mass yields and seed aerosol surface area. However,

125 the use of high seed aerosol surface area concentrations in chamber studies may

126 complicate the particle wall-loss correction since (depending on the particle wall-loss

127 correction method used) the role of coagulation may need to be accounted for. It also

128 needs to be established how particle wall-deposition rates may change when different
129 seed aerosol concentrations (i.e., number, surface area and volume concentrations) and
130 size distributions are used. These uncertainties underscore the need to better constrain the
131 uncertainties associated with particle wall-loss correction since this correction will affect
132 the evaluation of the magnitude by which vapor wall-loss impacts chamber-derived SOA
133 mass yields.

134 In this work, we present results from targeted chamber experiments demonstrating
135 the change of size-dependent particle wall-deposition rates with different seed aerosol
136 concentrations (i.e., number, surface area and volume concentrations) and size
137 distributions. We also demonstrate how coagulation can be (and needs to be) accounted
138 for in experiments in which high seed aerosol surface area concentrations are used to
139 promote the condensation of SOA-forming vapors onto seed aerosol. Finally, we
140 compare SOA mass concentrations and yields in the canonical α-pinene ozonolysis
141 system obtained using four different particle wall-deposition correction methods, and
142 examine the uncertainties associated with each method. This work builds on our previous
143 study on the influence of seed aerosol surface area concentration and hydrocarbon
144 oxidation rate on vapor wall deposition and SOA mass yields in the α-pinene ozonolysis
145 system (Nah et al., 2016). In our previous study, we used a coupled vapor-particle
146 dynamics model to show that the condensation of SOA-forming vapors onto seed aerosol
147 in the α-pinene ozonolysis system is dominated by quasi-equilibrium growth. This
148 present work is aimed at understanding the uncertainties in the SOA mass yields due to
149 the application of different particle wall-deposition correction methods.

150 **2. Experimental**

151 Experiments were carried out in the Georgia Tech Environmental Chamber
152 (GTEC) facility (Boyd et al., 2015). A single FEP Teflon chamber (volume 13 m^3) was
153 used for the entire study. Prior to each experiment, the chamber was flushed with dried,
154 purified air for > 24 h until the aerosol number concentration was < 30 cm^{-3}. Experiments
155 were performed at < 5 % RH and 25 °C. NO_x mixing ratios in these experiments were < 1
156 ppb.

157   The dark α-pinene ozonolysis experimental procedure used in this study was
158 similar to that used in Nah et al. (2016). First, 22 ppm of cyclohexane (Sigma Aldrich, ≥
159 99.9 %), which served as an OH scavenger (~440 times the initial α-pinene
160 concentration), was injected into the chamber. Based on the cyclohexane and α-pinene
161 concentrations in the chamber, the reaction rate of OH with cyclohexane is ~60 times
162 greater than that with α-pinene. Ammonium sulfate (AS) seed aerosol was next
163 introduced into the chamber via atomization of an aqueous AS solution. A known
164 concentration of α-pinene (Sigma Aldrich, > 99 %) (~50 ppb in all experiments) was then
165 injected into the chamber. Finally, 500 ppb of ozone (O_3), which was generated by
166 passing purified air into a photochemical cell (Jelight 610), was introduced into the
167 chamber for 54.25 min after the seed aerosol and α-pinene concentrations in the chamber
168 had stabilized. The beginning of O_3 injection into the chamber marked the start of the
169 reaction (i.e., reaction time = 0 min). The O_3 mixing timescale was ~12 min for all
170 experiments. The O_3 injection time and mixing timescale were determined from separate
171 O_3-only experiments (Nah et al., 2016). In seed-only experiments performed to measure
172 size-dependent particle wall-deposition coefficients, only AS seed aerosol was introduced
173 into the chamber. A gas chromatograph-flame ionization detector (GC-FID, Agilent
174 7890A) and O_3 monitor (Teledyne T400) measured the α-pinene and O_3 concentrations,
175 respectively. GC-FID measurements were taken 15 min apart. A high-resolution time-of-
176 flight aerosol mass spectrometer (HR-ToF-AMS, Aerodyne Research Inc.) measured the
177 aerosol elemental composition (DeCarlo et al., 2006; Canagaratna et al., 2015). A
178 scanning mobility particle sizer (SMPS, TSI), which consists of a differential mobility
179 analyzer (DMA, TSI 3081) and a condensation particle counter (CPC, TSI 3775),
180 measured the aerosol size distributions, number and volume concentrations.

181   The initial total AS seed aerosol surface area concentrations used in this study
182 were ~1000 and ≥ 8000 μm^2 cm^{-3} (referred to as "low-SA" and "high-SA" experiments,
183 respectively). To investigate how the seed aerosol size distribution may affect SOA mass
184 concentrations and yields, two different concentrations of AS solutions were used to
185 generate AS seed aerosol for both the seed-only and α-pinene ozonolysis experiments:
186 0.015 M or 0.05 M. In some experiments, both the 0.015 and 0.05 M AS solutions were
187 atomized into the chamber to achieve the desired total AS seed aerosol surface area

188 concentration. In these experiments, the 0.015 M AS solution was first atomized into the

189 chamber to achieve about half of the desired total AS seed aerosol surface area

190 concentration, followed by atomization of the 0.05 M AS solution. A summary of the

191 experimental conditions is shown in Table 1.

192 **3. Aerosol dynamics model**

193 An aerosol dynamics model is used to determine particle wall-deposition

194 coefficients that have been corrected for coagulation. This model was first described in

195 Pierce et al. (2008). In our work, we do not use the full Aerosol Parameter Estimation

196 (APE) model described in Pierce et al. (2008), but rather we ~~use~~ employ the model used

197 to create the "No condensation" curve in Fig. 5 of the paper. This model includes only

198 coagulation and particle wall-loss, and it assumes that no condensation or evaporation

199 occurs during seed-only experiments, which are especially designed to measure particle

200 wall-deposition rates (experiments 1 through 6 in Table 1). Coagulation coefficients are

201 calculated from Table 13.1 in Seinfeld and Pandis (2016). The inputs to the model are the

202 raw time-dependent number distribution data measured by the SMPS during a particular

203 seed-only experiment. For each time step of the SMPS measurements, the model

204 calculates the decrease in the number concentration in each particle size bin due solely to

205 coagulation. The difference between this calculated decrease and the observed decrease

206 in the number concentration is attributed to particle wall-deposition, thus allowing size-

207 dependent particle wall-deposition coefficients to be determined. The model then re-

208 calculates the decrease in the number concentration for each particle size bin for that time

209 step due to both coagulation and particle wall-deposition using the deposition coefficients

210 just determined. The calculated decrease in the number concentration is again compared

211 to the measured values. This process of finding the size-dependent particle wall-

212 deposition rates is iterated using Newton's method in order to converge upon particle

213 wall-deposition coefficients that fit the calculated number concentration decay to the

214 observed decay. The process is repeated for each SMPS measurement time step, yielding

215 size- and time-dependent particle wall-deposition coefficients. This process of finding the

216 size-dependent particle wall-deposition rates is carried out only when the number

217 concentration in the particle size bin of interest is > 20 particles cm^{-3}. For bins with ≤ 20

218   particles cm^{-3}, the deposition coefficient is not calculated during these time steps due to
219   uncertainties in the number counts in these bins leading to low confidence in the
220   determined particle wall-deposition rates. The deposition coefficients are averaged over
221   the entire experiment to yield coagulation-corrected size-dependent particle wall-
222   deposition coefficients.

223   **4. Results and discussion**

224   **4.1. Role of coagulation in particle wall-deposition corrections**

225   We performed a set of seed-only experiments using 0.015 M AS and/or 0.05 M
226   AS solutions to determine the extent to which size-dependent particle wall-loss rates
227   change with different seed aerosol concentrations and size distributions (experiments 1
228   through 6 in Table 1). The initial total AS seed aerosol surface area concentrations in the
229   low-SA-seed-only and high-SA-seed-only experiments are similar to those used in the α-
230   pinene ozonolysis experiments (i.e., ~1000 and $\geq$ 8000 μm^2 cm^{-3}, respectively). Figure S1
231   shows the initial and final (420 min) number and volume size distributions for the seed-
232   only experiments. The initial number and volume size distributions in the low-SA-seed-
233   only experiments are smaller than those in the high-SA-seed-only experiments, regardless
234   of the concentration of the AS solution used to generate seed aerosol. As expected, all of
235   the size distributions shift to larger particle diameters as the experiment progresses due to
236   more efficient loss of smaller particles to the chamber walls and via coagulation as
237   compared to larger particles.

238   Figure 1 shows the size-dependent particle wall-deposition coefficients measured
239   directly in the low-SA-seed-only and high-SA-seed-only experiments (dashed lines). We
240   will refer to them as the *uncorrected* size-dependent particle wall-deposition coefficients
241   for the remainder of the discussion in this work since the effect of coagulation is assumed
242   to be negligible, and thus coagulation is not corrected for in these coefficients. The
243   uncorrected size-dependent particle wall-deposition coefficients are obtained directly
244   from SMPS measurements by fitting a first-order exponential decay to the measured
245   particle number concentration decay in each size bin. The uncorrected particle wall-
246   deposition coefficients are compared to those corrected for coagulation (shown as solid

247   lines in Fig. 1), which are obtained from the application of the aerosol dynamics model

248   (described in section 3) to the number distribution data measured by the SMPS. As

249   anticipated, a comparison of the uncorrected and coagulation-corrected size-dependent

250   particle wall-deposition coefficients indicates that coagulation has a smaller effect on the

251   deposition coefficients from the low-SA-seed-only experiments (experiments 1 through

252   4) compared to the high-SA-seed-only experiments (experiments 5 and 6). For example,

253   for particle diameters > 400 nm, the coagulation-corrected deposition coefficients for the

254   high-SA-seed-only experiments are up to an order of magnitude faster than the

255   uncorrected deposition coefficients. The smaller uncorrected deposition coefficients can

256   be attributed to particle formation (via coagulation) occurring simultaneously with

257   particle wall-deposition at these larger particle diameters in the high-SA-seed-only

258   experiments. A comparison of the change in total particle number concentration due to

259   coagulation alone (Fig. S2) shows that the low-SA-seed-only experiments (experiments 1

260   through 4) have smaller coagulation rates than the high-SA-seed-only experiments

261   (experiments 5 and 6). The observation that coagulation has a smaller effect on the

262   inferred deposition coefficients in the low-SA-seed-only experiments is expected since

263   these experiments involve significantly smaller particle number concentrations as

264   compared to the high-SA-seed-only experiments (2.5 to 4 x 10^4 particles cm^{-3} vs. 1 to 1.3

265   x 10^5 particles cm^{-3}).

266   The coagulation-corrected size-dependent particle wall-deposition coefficients

267   obtained from the low-SA-seed-only experiments are generally in agreement. This is also

268   the case for the coagulation-corrected particle wall-deposition coefficients obtained from

269   the high-SA-seed-only experiments. Similar trends are observed for the uncorrected size-

270   dependent particle wall-deposition coefficients. Therefore, the concentration of the AS

271   solution(s) (i.e., 0.015 M and/or 0.05 M) used to generate the seed aerosol in seed-only

272   experiments does not influence the size-dependent particle wall-deposition coefficients.

273   The coagulation-corrected size-dependent particle wall-deposition coefficients obtained

274   from the low-SA-seed-only experiments are different from those obtained from the high-

275   SA-seed-only experiments. In addition, the minimum coagulation-corrected particle wall-

276   deposition coefficient for the low-SA-seed-only experiment (minimum particle diameter

277   ~300 nm) is lower than that of the high-SA-seed-only experiments (minimum particle

278 diameter ~530 nm). This result is surprising since the particle wall-deposition coefficients
279 are expected to depend solely on particle size once coagulation is accounted for.

280   We identify two possible explanations for the differences in the coagulation-
281 corrected particle wall-deposition coefficients. The first possibility is that there is a
282 difference in particle charging of the seed aerosol in the low-SA-seed-only and high-SA-
283 seed-only experiments. Particle wall-deposition is enhanced when charges are present on
284 particles (McMurry and Grosjean, 1985; McMurry and Rader, 1985; Pierce et al., 2008).
285 In all our experiments, a Boltzmann charge distribution was applied to the AS seed
286 aerosol by passing the particles through a Po-210 neutralizer prior to injection into the
287 chamber. However, it is possible that the particles are not fully neutralized before
288 entering the chamber, resulting in a difference in the true particle wall-deposition
289 coefficients due to the differences in particle charging between the experiments.

290   The second possible explanation for the differences in the coagulation-corrected
291 particle wall-deposition coefficients is that the Brownian coagulation kernel that we used
292 for our coagulation correction may not account for ~~all of~~ the entire coagulation rate in the
293 chamber. Coulombic and/or van der Walls forces may enhance the coagulation rates. We
294 performed a series of ~~simple~~ sensitivity tests to determine ~~how~~ the extent to which the
295 coagulation-corrected size-dependent particle wall-deposition coefficients change as a
296 function of coagulation coefficients. In these tests, we scale ~~our~~ the Brownian coagulation
297 kernel by 1.1 and 1.5 uniformly across all particle sizes (as Coulombic and van der Waals
298 enhancements to coagulation have size dependence, these simple sensitivity tests do not
299 fully capture the changes due to either of these forces). Figure S3 shows results from
300 sensitivity tests performed on the seed-only experiments. These sensitivity tests show that
301 the coagulation-corrected particle wall-deposition coefficients in the low-SA-seed-only
302 and high-SA-seed-only experiments converge towards each other with increasing scale
303 factors on coagulation. However, with increasing coagulation scale factors, our derived
304 wall-deposition coefficients become negative at some particle sizes, which implies that
305 the size-independent coagulation scale factors are unrealistic. Future work should include
306 a more detailed investigation of the size-dependent coagulation enhancements provided
307 by Coulombic and van der Waals forces (which in turn requires knowledge about the

308 charge distribution and van der Waals forces), and it should include an investigation of

309 the change-enhanced particle wall-losses (again requiring a knowledge of the charge

310 distribution). For the remainder of this work, we will use coagulation-corrected particle

311 wall-deposition coefficients with no enhancement to the coagulation rates (solid lines in

312 Figs. 1 and S3a).

313   We evaluated the effectiveness of the coagulation-corrected particle wall-

314 deposition coefficients (with no scaling of Brownian coagulation) in correcting for

315 particle wall-loss and coagulation by applying these coefficients to the SMPS data from

316 the seed-only experiments. The corrected volume concentration should level off at a

317 constant value (at the initial particle volume concentration) when particle wall-deposition

318 and coagulation are properly accounted for, since no condensation or evaporation occurs

319 during these experiments (due to the use of low-volatility AS seed aerosol and the

320 absence of condensable gases) and the wall-deposited particle volume concentration is

321 added back to the suspended particle volume concentration during particle wall-loss

322 correction. Figure S4 shows the raw and particle wall-deposition-corrected volume

323 concentrations. Coagulation-corrected size-dependent particle wall-deposition

324 coefficients are used for the particle wall-deposition correction shown in Fig. S4. Over all

325 experiments, the particle wall-deposition-corrected final volume concentration (i.e., at the

326 end of the experiment) is within 1 to 5 % of the initial volume concentration (Table S1).

327 **4.2. α-pinene ozonolysis**

328   We use the "size-dependent" method described in Loza et al. (2012) and Nah et

329 al. (2016) to correct for particle wall-deposition in the α-pinene ozonolysis experiments.

330 Briefly, size-dependent particle wall-deposition coefficients determined in separate seed-

331 only experiments (either through direct measurements or using an aerosol dynamics

332 model) are used to correct for particle wall-deposition in SOA-formation experiments.

333 Here we assume that particles cease to uptake SOA-forming vapors once they have

334 deposited, and hence the SOA mass present on deposited particles does not increase after

335 deposition. A key assumption of the "size-dependent" method is that the size-dependent

336 particle wall-deposition coefficients do not change significantly between experiments.

337 Seed-only experiments are performed regularly in the GTEC chamber. As shown in Fig.

338 1 (and Fig. 1 of Nah et al. (2016)), the uncorrected and coagulation-corrected size-
339 dependent particle wall-deposition coefficients are generally in line with each other at a
340 given seed aerosol surface area concentration. Since the seed-only and α-pinene
341 ozonolysis experiments were performed under similar experimental conditions (i.e., dark
342 conditions at < 5 % RH and 25 °C), the size-dependent particle wall-deposition
343 coefficients are not expected to change significantly with reaction conditions for the
344 experiments presented in this study.

345   Since the focus of this work is the influence of coagulation and particle wall-
346 deposition on SOA mass yields, more high-SA α-pinene ozonolysis experiments
347 (experiments 9 through 12) were performed than low-SA experiments (experiments 7 and
348 8). To investigate the influence of coagulation on the SOA mass yields, both the
349 uncorrected and coagulation-corrected size-dependent particle wall-deposition
350 coefficients are used to correct for particle wall-deposition in the α-pinene ozonolysis
351 experiments. All the low-SA α-pinene ozonolysis data are particle wall-deposition-
352 corrected using uncorrected and coagulation-corrected size-dependent particle wall-
353 deposition coefficients from the low-SA-seed-only experiments, and all the high-SA α-
354 pinene ozonolysis data are corrected using uncorrected and coagulation-corrected particle
355 wall-deposition coefficients from the high-SA-seed-only experiments. Additional details
356 regarding the size-dependent particle wall-deposition coefficients used to correct for
357 particle wall-deposition in the different α-pinene ozonolysis experiments are provided in
358 Table 1. Figure S5 shows the raw and particle wall-deposition-corrected aerosol volume
359 concentrations for all the α-pinene ozonolysis experiments. In all the α-pinene ozonolysis
360 experiments, the volume concentrations that have been particle wall-deposition-corrected
361 using coagulation-corrected size-dependent particle wall-deposition coefficients (black)
362 reach peak values at reaction time ~100 min. In contrast, volume concentrations that have
363 been particle wall-deposition-corrected using uncorrected size-dependent particle wall-
364 deposition coefficients (blue) increase monotonically in the high-SA experiments
365 (experiments 9 through 12).

366   The SOA mass concentration is calculated from the product of the SOA density
367 with the difference of the particle wall-deposition-corrected volume concentration and the

368   initial seed aerosol volume concentration. We use an SOA density of 1.37 g cm^{-3}, which

369   was previously measured by Nah et al. (2016). Figure 2 shows the reaction profiles of the

370   low-SA α-pinene ozonolysis experiments. The SOA mass concentrations obtained using

371   the coagulation-corrected (Figs. 2a and 2b) and uncorrected (Figs. 2c and 2d) size-

372   dependent particle wall-deposition coefficients are sufficiently similar, which suggests

373   that coagulation plays a minor role in the low-SA experiments. As reported in Nah et al.

374   (2016), SOA growth typically occurs within 10 to 20 min of the start of the reaction. The

375   molar ratio of O$_3$ reacted to α-pinene reacted is approximately 1:1 (i.e., 50 ppb α-pinene

376   reacted with 50 ppb O$_3$), which indicates that O$_3$ reacts with α-pinene and not its

377   oxidation products. All the α-pinene reacts within 90 to 100 min of the start of reaction in

378   the 500 ppb O$_3$ experiments, and peak SOA levels occur at reaction time ~100 min. SOA

379   growth basically ceases once all the α-pinene has reacted, indicating that the first step of

380   α-pinene ozonolysis is rate-limiting and the first-generation products are condensable (

381   Gao et al., 2004a and 2004b; Ng et al., 2006; Chan et al., 2007). This result is expected

382   since α-pinene has a single double bond. The slight decrease in the SOA mass

383   concentrations after peak SOA growth may be due to imperfections in the particle wall-

384   deposition correction and/or vapor wall-deposition.

385   Figure 3 shows the reaction profiles of the high-SA α-pinene ozonolysis

386   experiments. In cases where the coagulation-corrected size-dependent particle wall-

387   deposition coefficients are used to correct for particle wall-deposition (Figs. 3a-d), the

388   SOA growth profile is similar to that of the low-SA experiments; SOA growth essentially

389   stops once all the α-pinene has reacted, as expected (Gao et al., 2004a and 2004b; Ng et

390   al. 2006; Chan et al., 2007). In contrast, when the uncorrected size-dependent particle

391   wall-deposition coefficients are used to correct for particle wall-deposition (Figs. 3e-h),

392   the SOA mass concentration continues to increase even after all the α-pinene has reacted.

393   This indicates that for the "size-dependent" method, SOA mass concentrations, and

394   consequently SOA mass yields, can be substantially overestimated when coagulation is

395   not accounted for during particle wall-deposition correction in high-SA experiments. This

396   underscores the importance of accounting for coagulation and particle wall-deposition

397   appropriately in chamber studies that employ high seed aerosol concentrations. We will

398   use SOA mass concentrations corrected using coagulation-corrected size-dependent

399   particle wall-deposition coefficients (solid lines in Fig. 1) for the remainder of the
400   discussion in this work.

401   Figure 4 shows the time-dependent SOA mass yields as a function of initial seed
402   aerosol surface area concentration for the α-pinene ozonolysis experiments. Also
403   included in Fig. 4 are results from Nah et al. (2016); SOA mass concentrations obtained
404   using coagulation-corrected size-dependent particle wall-deposition coefficients
405   determined in their study (Fig. S7 of Nah et al. (2016)). The SOA mass yield at peak
406   SOA growth remains approximately constant even at seed aerosol surface area
407   concentrations ≥ 8000 μm^2 cm^{-3}. This confirms conclusions from our previous study that
408   the seed aerosol surface area concentration does not influence the partitioning of gas-
409   phase products to the particle phase in the α-pinene ozonolysis system (Nah et al., 2016).
410   As discussed in Nah et al. (2016), this behavior arises because SOA formation in the α-
411   pinene ozonolysis system is dominated by quasi-equilibrium growth (Saleh et al., 2013),
412   which occurs when the production rate of SOA-forming vapors is significantly slower
413   than that required to establish gas-particle equilibrium (Riipinen et al., 2011; Shiraiwa
414   and Seinfeld, 2012; Zhang et al., 2012). Gas-particle equilibrium is governed by the
415   amount of organic material in the system when the vapor and particle phases maintain
416   equilibrium. Thus, the seed aerosol surface area does not control the condensation rate of
417   SOA-forming vapors (McVay et al., 2014).

418   It is important to note that when the uncorrected size-dependent particle wall-
419   deposition coefficients (dashed lines in Fig. 1) are used for the particle wall-deposition
420   correction, the predicted SOA mass yield at peak SOA growth increases with seed
421   aerosol surface area (Fig. S6). This trend would lead to the incorrect conclusion that SOA
422   formation in the α-pinene ozonolysis system is governed by kinetically limited growth.
423   Therefore, this result further highlights the importance of accounting for coagulation and
424   particle wall-deposition properly in chamber studies (especially when high number
425   concentrations of seed aerosol are used) to avoid erroneous conclusions regarding the role
426   of gas-particle partitioning (quasi-equilibrium vs. kinetically limited SOA growth) in
427   affecting vapor wall-deposition and SOA mass yields in VOC systems.

428   **4.3. Uncertainties in SOA mass concentrations due to particle wall-loss corrections**

429   In the previous section, we showed that ignoring the role of coagulation in the

430   "size-dependent" particle wall-deposition correction method can contribute significant

431   errors to the calculated SOA mass concentrations and yields. These uncertainties could

432   lead to erroneous conclusions regarding the role of gas-particle partitioning in influencing

433   vapor wall-loss in the VOC system. Here, we investigate the uncertainties in the SOA

434   mass concentrations and yields as a result of the use of different particle wall-deposition

435   correction methods. We analyzed data from the α-pinene ozonolysis experiments using

436   four different commonly used particle wall-deposition correction methods. SOA mass

437   concentrations and yields obtained using the "size-dependent" particle wall-deposition

438   correction method (discussed in section 4.2) are compared to those obtained using the

439   "number averaged", "volume averaged" and "inert tracer" methods, which are described

440   previously by Carter et al. (2005), Pathak et al. (2008) and Hildebrandt et al. (2009),

441   respectively. For the "size-dependent" method, only SOA mass concentrations and yields

442   corrected using coagulation-corrected size-dependent particle wall-deposition coefficients

443   (Fig. 4) will be used in the discussion presented here.

444   The "number averaged" and "volume averaged" methods use SMPS

445   measurements taken during SOA-formation studies. The "number averaged" method

446   involves measuring the average loss rate of the total aerosol number concentration after

447   peak SOA growth and then applying this first-order particle wall-deposition rate to the

448   entire experiment to correct for particle wall-loss (Carter et al., 2005). Since the average

449   loss rate of the total aerosol volume concentration is assumed to be the same as that of the

450   total aerosol number concentration, this first-order particle wall-deposition rate is also

451   applied to the total aerosol volume concentration data to determine the SOA mass

452   concentration. The "volume averaged" method involves measuring the average loss rate

453   of the total aerosol volume or mass concentration after peak SOA growth, and then

454   applying this first-order particle wall-deposition rate to the entire experiment to correct

455   for particle wall-loss (Pathak et al., 2007). Since the particle wall-deposition rate is

456   directly measured during SOA-formation experiments in the "number averaged" and

457   "volume averaged" methods, day-to-day variations of the particle wall-deposition rates

458   are accounted for. Unlike the "size-dependent" method, the "number averaged" and

459   "volume averaged" methods assume that particle wall-deposition rates depend weakly on

460 particle size, and hence particle wall-deposition can be represented by a single first-order

461 decay rate constant (Carter et al., 2005; Pathak et al., 2007; Pierce et al., 2008). It is

462 currently unclear if this assumption is valid for all seed aerosol concentrations (i.e.,

463 number, surface area and volume concentrations). The "inert tracer" method can be used

464 in SOA-formation studies where SMPS and AMS measurements are taken and non-

465 volatile sulfate seed aerosol is used (Hildebrandt et al., 2009). The SOA mass

466 concentration is calculated from the product of the initial seed aerosol sulfate mass

467 concentration (measured by the SMPS) to the time-dependent organic-to-sulfate

468 (Org/SO$_4$) ratio (measured by the HR-ToF-AMS). Examples of the application of the

469 "number averaged", "volume averaged" and "inert tracer" methods to the α-pinene

470 ozonolysis data are shown in Fig. S7.

471   In original descriptions of the "size-dependent", "number averaged" and "volume

472 averaged" methods, the authors assumed that particles cease to uptake SOA-forming

473 vapors once they have deposited to the walls, thus the SOA mass present on deposited

474 particles does not increase after deposition (Carter et al., 2005; Pathak et al., 2007; Loza

475 et al., 2012). In contrast, the "inert tracer" method assumes that deposited particles

476 continue to uptake suspended SOA-forming vapors at similar rates as suspended

477 particles, and hence the SOA mass present on the deposited particles will increase at the

478 same rate as those suspended (Hildebrandt et al., 2009). Therefore, SOA mass

479 concentrations and yields calculated by the "inert tracer" method are expected to be

480 higher than that calculated using the original descriptions of the "size-dependent",

481 "number averaged" and "volume averaged" methods. It is important to note that the

482 assumption that deposited particles continue to uptake suspended SOA-forming vapors at

483 similar rates as suspended particles can also be applied to the "size-dependent", "number

484 averaged" and "volume averaged" methods, which in turn will result in higher calculated

485 SOA mass concentrations and yields. However, we will use the "size-dependent",

486 "number averaged" and "volume averaged" methods as originally described by Loza et

487 al. (2012), Carter et al. (2005) and Pathak et al. (2007), respectively, to correct for

488 particle wall-deposition in this discussion (i.e., deposited particles do not uptake SOA-

489 forming vapors). The "inert tracer" method will be used to evaluate its ability to predict

490 the role of gas-particle partitioning (quasi-equilibrium vs. kinetically limited SOA

491   growth) in affecting vapor wall-deposition and SOA mass yields in the α-pinene

492   ozonolysis system.

493   Figure 5 shows the SOA mass concentrations as a function of reaction time for the

494   four particle wall-deposition correction methods. For the low-SA experiments (Figs. 5a

495   and 5b), the SOA growth profiles obtained using the four different particle wall-

496   deposition correction methods are similar; SOA growth virtually stops after all the α-

497   pinene has reacted (at reaction time ~90 to 100 min). As expected, the SOA mass

498   concentrations calculated by the "inert tracer" method are higher than the SOA mass

499   concentrations calculated by the "size-dependent", "number averaged" and "volume

500   averaged" methods. The SOA mass concentrations calculated by the "size-dependent",

501   "number averaged" and "volume averaged" particle wall-deposition methods are

502   generally consistent with each other.

503   For the high-SA experiments (Figs. 5c to 5f), the SOA mass concentrations

504   calculated using the "size-dependent", "volume averaged" and "inert tracer" methods

505   stop increasing after all the α-pinene has reacted (at reaction time ~90 to 100 min). In

506   contrast, the SOA mass concentrations calculated using the "number averaged" method

507   continued to increase even after all the α-pinene has reacted. These results suggest that

508   the calculated SOA mass concentrations and yields will be substantially overestimated if

509   the "number averaged" method is used to correct for particle wall-deposition in

510   experiments where high seed aerosol surface area concentrations are used. The erroneous

511   increase in the SOA mass concentration calculated by the "number averaged" method can

512   be attributed to the method's assumption that the average loss rate of the total aerosol

513   volume concentration is the same as that of the total aerosol number concentration. The

514   "number averaged" method is effective in experiments where low concentrations of seed

515   aerosol are used since coagulation plays a minor role in affecting the average loss rate of

516   the total aerosol number concentration. However, it loses its accuracy in experiments

517   under high seed aerosol number concentrations because the average loss rate of the total

518   aerosol number concentration is driven by both coagulation and particle wall-deposition.

519   It is possible that the "number averaged" method may be an effective particle wall-

520   deposition correction method in these experiments if the measurements are corrected for

521   coagulation. The effect of coagulation on the SOA mass concentrations calculated by the

522   "volume averaged" and "inert tracer" methods is less prominent since coagulation does

523   not affect the aerosol volume and mass concentrations. Together, our results indicate that

524   the "size-dependent" (when coagulation is accounted for), "volume averaged" and "inert

525   tracer" methods are effective particle wall-deposition correction methods (regardless of

526   seed aerosol surface area concentrations) since the calculated SOA mass concentrations

527   stopped increasing after all the α-pinene has reacted.

528   Figure 6 shows the time-dependent SOA mass yields as a function of initial total

529   AS seed aerosol surface area concentration for the "number averaged", "volume

530   averaged" and "inert tracer" particle wall-deposition correction methods. Also shown in

531   Fig. 6 are time-dependent SOA mass yields calculated using these three methods for the

532   α-pinene ozonolysis raw data reported by Nah et al. (2016). The time-dependent SOA

533   mass yields for the "number averaged", "volume averaged" and "inert tracer" methods

534   (Fig. 6) are compared to those calculated using the "size-dependent" method (Fig. 4). For

535   seed aerosol surface area concentrations < 3000 μm^2 cm^{-3}, the SOA mass yields at peak

536   SOA growth (absolute values) calculated by the "size-dependent", "number averaged"

537   and "volume averaged" methods agree within 14 % (Figs. 4, 6a and 6b). In contrast, for

538   seed aerosol surface area concentrations ≥ 8000 μm^2 cm^{-3}, the SOA mass yields at peak

539   SOA growth calculated by the "number averaged" method range from 70.8 to 76.5 %

540   (Fig. 6a), while SOA mass yields at peak SOA growth calculated by the "size-dependent"

541   and "volume averaged" methods range from 17.2 to 27 % (Figs. 4 and 6b). As discussed

542   previously, this disagreement in the SOA mass yields is due to the treatment of (or lack

543   thereof) coagulation in the "number averaged" method. Failure to account for coagulation

544   in the "number averaged" method also resulted in the calculated SOA mass yields

545   increasing with seed aerosol surface area (Fig. 6a), which could lead to the incorrect

546   conclusion that SOA formation in the α-pinene ozonolysis system is governed by

547   kinetically limited growth. In contrast, the SOA mass yields calculated by the "volume

548   averaged" and "inert tracer" methods remain roughly constant despite the increase in AS

549   seed aerosol surface area (Figs. 6b and 6c), consistent with the results obtained using the

550   "size-dependent" method (Fig. 4).

5. Conclusions

An aerosol dynamics model can be used to account for coagulation in chamber studies in which large seed aerosol surface area concentrations are used. Coagulation-corrected size-dependent particle wall-deposition coefficients are obtained from the application of the aerosol dynamics model to the experimental data from seed-only experiments. Using these coagulation-corrected size-dependent particle wall-deposition coefficients, we showed that the α-pinene ozonolysis SOA mass yields at peak SOA growth remain approximately constant even when very high seed aerosol surface area concentrations (≥ 8000 μm^2 cm^{-3}) are used. This confirms conclusions from our previous study that the seed aerosol surface area concentration does not influence the partitioning of α-pinene ozonolysis gas-phase products to the particle phase (Nah et al., 2016). Thus, this indicates that SOA formation in the α-pinene ozonolysis system is dominated by quasi-equilibrium growth, and that there are no significant limitations to vapor-particle mass transfer (McVay et al., 2014; Nah et al., 2016).

The variability in the calculated SOA mass concentrations and yields between four different particle wall-deposition correction methods is also evaluated for a series of α-pinene ozonolysis experiments. In the experiments with low seed aerosol surface area concentrations (< 3000 μm^2 cm^{-3}), the SOA mass yields obtained by the different particle wall-deposition correction methods (i.e., the "size-dependent", "number averaged" and "volume averaged" methods) are generally consistent with one another. This indicates that these three methods are effective in correcting for particle wall-deposition in experiments that use low seed aerosol surface area concentrations. However, in the experiments with high seed aerosol surface area concentrations (≥ 8000 μm^2 cm^{-3}), the calculated SOA mass yields differ substantially. These differences arise from assumptions made in the particle wall-deposition correction method regarding the influence of coagulation on the first-order particle wall-loss rate. Specifically, we find that coagulation needs to be accounted for in the "size-dependent" and "number averaged" methods in order for them to be effective in chamber studies that use high seed aerosol surface area concentrations. Coagulation does not need to be accounted for in the

580   "volume averaged" method since coagulation does not affect aerosol volume
581   concentrations.

582   Chamber experiments are subject to both particle and vapor wall-deposition.
583   While understanding the effect of vapor wall-deposition on the SOA mass yields is
584   critical, SOA mass yield uncertainties introduced by the particle wall-deposition
585   correction cannot be neglected. Results from this study underscore the importance of
586   constraining the SOA mass yield uncertainties introduced by the particle wall-deposition
587   correction regardless of the VOC system. Specifically, the effect of coagulation on
588   particle wall-deposition rates can be an important source of uncertainty not only in
589   determining SOA mass concentrations and yields, but also in evaluating the role of gas-
590   particle partitioning (quasi-equilibrium vs. kinetically limited SOA growth) in affecting
591   vapor wall-deposition in VOC systems. Here we showed that the condensation of SOA-
592   forming vapors in the α-pinene ozonolysis system can be erroneously concluded as
593   kinetically limited if coagulation is not accounted for in the "size-dependent" and
594   "number averaged" particle wall-deposition correction methods. Similar flawed
595   conclusions in other VOC systems may be drawn in chamber studies that use high seed
596   aerosol surface area concentrations to promote SOA formation but do not account for
597   coagulation. Therefore, we recommend accounting for coagulation when the "size-
598   dependent" and "number averaged" particle wall-deposition correction methods are used
599   in chamber studies that use high seed aerosol surface area concentrations (~~i.e.~~e.g., ≥ 3000
600   μm^2 cm^{-3}) to promote the condensation of SOA-forming vapors onto seed aerosol
601   regardless of VOC system. Alternatively, the "volume averaged" and "inert tracer"
602   methods can be used in chamber studies that use high seed aerosol surface area
603   concentrations. In addition, we suggest using multiple techniques (i.e., at least 2) to
604   correct for particle wall-loss in order to determine the effect of SOA mass yield
605   uncertainties introduced by particle wall-deposition correction. Complications arising
606   from particle and vapor wall deposition may also be potentially minimized by conducting
607   shorter duration chamber experiments. This can be achieved by using excess oxidant
608   concentrations, which increase the oxidation rate, and consequently reduce the time at
609   which peak SOA growth is achieved (Nah et al., 2016).

610   It is important to note that while results from the present study indicate that the

611 "volume ~~dependent~~averaged" and "inert tracer" methods are appropriate particle wall-

612 deposition correction methods for SOA-formation studies (regardless of seed aerosol

613 surface area concentrations) performed in the GTEC chamber in which the particle wall-

614 loss rates strongly depend on particle size, this may not be the case for all chambers. In

615 addition to particle size, particle wall-deposition rates depend on the chamber geometry,

616 chamber turbulence induced by mixing, and charge distribution on particles (Crump and

617 Seinfeld, 1981; McMurry and Rader, 1985). All these factors need to be considered

618 before one decides which particle wall-deposition correction method to use in SOA-

619 formation studies. It is possible that the "volume averaged~~dependent~~" and "inert tracer"

620 methods may not be appropriate particle wall-deposition correction methods for SOA-

621 formation studies performed in a chamber in which the particle wall-loss rates are even

622 more strongly dependent on particle size compared to the GTEC chamber. Therefore, we

623 recommend performing at least one separate seed-only experiment to measure the size-

624 dependent particle wall-deposition coefficients in order to probe the particle wall-

625 deposition characteristics of the chamber used before deciding on the particle wall-

626 deposition method to use in SOA-formation studies.

627 **Acknowledgements**

628   This research was funded by NSF grants 1455588 and AGS-1523500, and US

629 Environmental Protection Agency STAR grant (Early Career) RD-83540301. This

630 publication's contents are solely the responsibility of the grantee and do not necessarily

631 represent the official views of the US EPA. Further, US EPA does not endorse the

632 purchase of any commercial products or services mentioned in the publication. R.C.

633 McVay was supported by a National Science Foundation Graduate Research Fellowship

634 under grant No. DGE-1144469.

635 **References**

636 Boyd, C. M., Sanchez, J., Xu, L., Eugene, A. J., Nah, T., Tuet, W. Y., Guzman, M. I., and

637 Ng, N. L.: Secondary organic aerosol formation from the β-pinene+NO3 system: effect of

638   humidity and peroxy radical fate, Atmos. Chem. Phys., 15, 7497-7522, 10.5194/acp-15-

639   7497-2015, 2015.

640   Canagaratna, M. R., Jimenez, J. L., Kroll, J. H., Chen, Q., Kessler, S. H., Massoli, P.,

641   Hildebrandt Ruiz, L., Fortner, E., Williams, L. R., Wilson, K. R., Surratt, J. D., Donahue,

642   N. M., Jayne, J. T., and Worsnop, D. R.: Elemental ratio measurements of organic

643   compounds using aerosol mass spectrometry: characterization, improved calibration, and

644   implications, Atmos. Chem. Phys., 15, 253-272, 10.5194/acp-15-253-2015, 2015.

645   Cappa, C. D., Jathar, S. H., Kleeman, M. J., Docherty, K. S., Jimenez, J. L., Seinfeld, J.

646   H., and Wexler, A. S.: Simulating secondary organic aerosol in a regional air quality

647   model using the statistical oxidation model – Part 2: Assessing the influence of vapor

648   wall losses, Atmos. Chem. Phys., 16, 3041-3059, 10.5194/acp-16-3041-2016, 2016.

649   Carter, W. P. L., Cocker, D. R., Fitz, D. R., Malkina, I. L., Bumiller, K., Sauer, C. G.,

650   Pisano, J. T., Bufalino, C., and Song, C.: A new environmental chamber for evaluation of

651   gas-phase chemical mechanisms and secondary aerosol formation, Atmospheric

652   Environment, 39, 7768-7788, 10.1016/j.atmosenv.2005.08.040, 2005.

653   Chan, A. W. H., Kroll, J. H., Ng, N. L., and Seinfeld, J. H.: Kinetic modeling of

654   secondary organic aerosol formation: effects of particle- and gas-phase reactions of

655   semivolatile products, Atmospheric Chemistry and Physics, 7, 4135-4147, 2007.

656   Cocker, D. R., Flagan, R. C., and Seinfeld, J. H.: State-of-the-art chamber facility for

657   studying atmospheric aerosol chemistry, Environmental Science & Technology, 35,

658   2594-2601, 10.1021/es0019169, 2001.

659   Crump, J. G., and Seinfeld, J. H.: Turbulent Deposition and Gravitational Sedimentation

660   of an Aerosol in a Vessel of Arbitrary Shape, Journal of Aerosol Science, 12, 405-415,

661   10.1016/0021-8502(81)90036-7, 1981.

662   DeCarlo, P. F., Kimmel, J. R., Trimborn, A., Northway, M. J., Jayne, J. T., Aiken, A. C.,

663   Gonin, M., Fuhrer, K., Horvath, T., Docherty, K. S., Worsnop, D. R., and Jimenez, J. L.:

Field-deployable, high-resolution, time-of-flight aerosol mass spectrometer, Analytical Chemistry, 78, 8281-8289, 10.1021/ac061249n, 2006.

Gao, S., Ng, N. L., Keywood, M., Varutbangkul, V., Bahreini, R., Nenes, A., He, J. W., Yoo, K. Y., Beauchamp, J. L., Hodyss, R. P., Flagan, R. C., and Seinfeld, J. H.: Particle phase acidity and oligomer formation in secondary organic aerosol, Environmental Science & Technology, 38, 6582-6589, 10.1021/es049125k, 2004a.

Gao, S., Keywood, M., Ng, N. L., Surratt, J., Varutbangkul, V., Bahreini, R., Flagan, R. C., and Seinfeld, J. H.: Low-molecular-weight and oligomeric components in secondary organic aerosol from the ozonolysis of cycloalkenes and alpha-pinene, J. Phys. Chem. A, 108, 10147-10164, 10.1021/jp047466e, 2004b.

Hallquist, M., Wenger, J. C., Baltensperger, U., Rudich, Y., Simpson, D., Claeys, M., Dommen, J., Donahue, N. M., George, C., Goldstein, A. H., Hamilton, J. F., Herrmann, H., Hoffmann, T., Iinuma, Y., Jang, M., Jenkin, M. E., Jimenez, J. L., Kiendler-Scharr, A., Maenhaut, W., McFiggans, G., Mentel, T. F., Monod, A., Prevot, A. S. H., Seinfeld, J. H., Surratt, J. D., Szmigielski, R., and Wildt, J.: The formation, properties and impact of secondary organic aerosol: current and emerging issues, Atmospheric Chemistry and Physics, 9, 5155-5236, 2009.

Hildebrandt, L., Donahue, N. M., and Pandis, S. N.: High formation of secondary organic aerosol from the photo-oxidation of toluene, Atmospheric Chemistry and Physics, 9, 2973-2986, 2009.

Kanakidou, M., Seinfeld, J. H., Pandis, S. N., Barnes, I., Dentener, F. J., Facchini, M. C., Van Dingenen, R., Ervens, B., Nenes, A., Nielsen, C. J., Swietlicki, E., Putaud, J. P., Balkanski, Y., Fuzzi, S., Horth, J., Moortgat, G. K., Winterhalter, R., Myhre, C. E. L., Tsigaridis, K., Vignati, E., Stephanou, E. G., and Wilson, J.: Organic aerosol and global climate modelling: a review, Atmospheric Chemistry and Physics, 5, 1053-1123, 2005.

Keywood, M. D., Varutbangkul, V., Bahreini, R., Flagan, R. C., and Seinfeld, J. H.: Secondary organic aerosol formation from the ozonolysis of cycloalkenes and related

691   compounds, Environmental Science & Technology, 38, 4157-4164, 10.1021/es035363o,
692   2004.

693   Kokkola, H., Yli-Pirila, P., Vesterinen, M., Korhonen, H., Keskinen, H., Romakkaniemi,
694   S., Hao, L., Kortelainen, A., Joutsensaari, J., Worsnop, D. R., Virtanen, A., and Lehtinen,
695   K. E. J.: The role of low volatile organics on secondary organic aerosol formation,
696   Atmospheric Chemistry and Physics, 14, 1689-1700, 10.5194/acp-14-1689-2014, 2014.

697   Krechmer, J. E., Pagonis, D., Ziemann, P. J., and Jimenez, J. L.: Quantification of Gas-
698   Wall Partitioning in Teflon Environmental Chambers Using Rapid Bursts of Low-
699   Volatility Oxidized Species Generated in Situ, Environmental Science & Technology, 50,
700   5757-5765, 10.1021/acs.est.6b00606, 2016.

701   Kroll, J. H., and Seinfeld, J. H.: Chemistry of secondary organic aerosol: Formation and
702   evolution of low-volatility organics in the atmosphere, Atmospheric Environment, 42,
703   3593-3624, 10.1016/j.atmosenv.2008.01.003, 2008.

704   La, Y. S., Camredon, M., Ziemann, P. J., Valorso, R., Matsunaga, A., Lannuque, V., Lee-
705   Taylor, J., Hodzic, A., Madronich, S., and Aumont, B.: Impact of chamber wall loss of
706   gaseous organic compounds on secondary organic aerosol formation: explicit modeling
707   of SOA formation from alkane and alkene oxidation, Atmos. Chem. Phys., 16, 1417-
708   1431, 10.5194/acp-16-1417-2016, 2016.

709   Loza, C. L., Chan, A. W. H., Galloway, M. M., Keutsch, F. N., Flagan, R. C., and
710   Seinfeld, J. H.: Characterization of Vapor Wall Loss in Laboratory Chambers,
711   Environmental Science & Technology, 44, 5074-5078, 10.1021/es100727v, 2010.

712   Loza, C. L., Chhabra, P. S., Yee, L. D., Craven, J. S., Flagan, R. C., and Seinfeld, J. H.:
713   Chemical aging of m-xylene secondary organic aerosol: laboratory chamber study,
714   Atmospheric Chemistry and Physics, 12, 151-167, 10.5194/acp-12-151-2012, 2012.

715   Matsunaga, A., and Ziemann, P. J.: Gas-Wall Partitioning of Organic Compounds in a
716   Teflon Film Chamber and Potential Effects on Reaction Product and Aerosol Yield

717   Measurements, Aerosol Science and Technology, 44, 881-892,
718   10.1080/02786826.2010.501044, 2010.

719   McMurry, P. H., and Grosjean, D.: Gas and Aerosol Wall Losses in Teflon Film Smog
720   Chambers, Environmental Science & Technology, 19, 1176-1182, 10.1021/es00142a006,
721   1985.

722   McMurry, P. H., and Rader, D. J.: Aerosol Wall Losses in Electrically Charged
723   Chambers, Aerosol Science and Technology, 4, 249-268, 10.1080/02786828508959054,
724   1985.

725   McVay, R. C., Cappa, C. D., and Seinfeld, J. H.: Vapor-Wall Deposition in Chambers:
726   Theoretical Considerations, Environmental Science & Technology, 48, 10251-10258,
727   10.1021/es502170j, 2014.

728   McVay, R. C., Zhang, X., Aumont, B., Valorso, R., Camredon, M., La, Y. S., Wennberg,
729   P. O., and Seinfeld, J. H.: SOA formation from the photooxidation of α-pinene:
730   systematic exploration of the simulation of chamber data, Atmos. Chem. Phys., 16, 2785-
731   2802, 10.5194/acp-16-2785-2016, 2016.

732   Nah, T., McVay, R. C., Zhang, X., Boyd, C. M., Seinfeld, J. H., and Ng, N. L.: Influence
733   of seed aerosol surface area and oxidation rate on vapor wall deposition and SOA mass
734   yields: a case study with α-pinene ozonolysis, Atmos. Chem. Phys., 16, 9361-9379,
735   10.5194/acp-16-9361-2016, 2016.

736   Ng, N. L., Kroll, J. H., Keywood, M. D., Bahreini, R., Varutbangkul, V., Flagan, R. C.,
737   Seinfeld, J. H., Lee, A., and Goldstein, A. H.: Contribution of first- versus second-
738   generation products to secondary organic aerosols formed in the oxidation of biogenic
739   hydrocarbons, Environmental Science & Technology, 40, 2283-2297,
740   10.1021/es052269u, 2006.

741   Odum, J. R., Hoffmann, T., Bowman, F., Collins, D., Flagan, R. C., and Seinfeld, J. H.:
742   Gas/Particle Partitioning and Secondary Organic Aerosol Yields, Environmental Science
743   & Technology, 30, 2580-2585, 10.1021/es950943+, 1996.

744 Odum, J. R., Jungkamp, T. P. W., Griffin, R. J., Flagan, R. C., and Seinfeld, J. H.: The
745 atmospheric aerosol-forming potential of whole gasoline vapor, Science, 276, 96-99,
746 10.1126/science.276.5309.96, 1997a.

747 Odum, J. R., Jungkamp, T. P. W., Griffin, R. J., Forstner, H. J. L., Flagan, R. C., and
748 Seinfeld, J. H.: Aromatics, reformulated gasoline, and atmospheric organic aerosol
749 formation, Environmental Science & Technology, 31, 1890-1897, 10.1021/es960535l,
750 1997b.

751 Pathak, R. K., Stanier, C. O., Donahue, N. M., and Pandis, S. N.: Ozonolysis of alpha-
752 pinene at atmospherically relevant concentrations: Temperature dependence of aerosol
753 mass fractions (yields), J. Geophys. Res.-Atmos., 112, 8, 10.1029/2006jd007436, 2007.

754 Pierce, J. R., Engelhart, G. J., Hildebrandt, L., Weitkamp, E. A., Pathak, R. K., Donahue,
755 N. M., Robinson, A. L., Adams, P. J., and Pandis, S. N.: Constraining particle evolution
756 from wall losses, coagulation, and condensation-evaporation in smog-chamber
757 experiments: Optimal estimation based on size distribution measurements, Aerosol
758 Science and Technology, 42, 1001-1015, 10.1080/02786820802389251, 2008.

759 Riipinen, I., Pierce, J. R., Yli-Juuti, T., Nieminen, T., Häkkinen, S., Ehn, M., Junninen,
760 H., Lehtipalo, K., Petäjä, T., Slowik, J., Chang, R., Shantz, N. C., Abbatt, J., Leaitch, W.
761 R., Kerminen, V. M., Worsnop, D. R., Pandis, S. N., Donahue, N. M., and Kulmala, M.:
762 Organic condensation: a vital link connecting aerosol formation to cloud condensation
763 nuclei (CCN) concentrations, Atmos. Chem. Phys., 11, 3865-3878, 10.5194/acp-11-3865-
764 2011, 2011.

765 Saleh, R., Donahue, N. M., and Robinson, A. L.: Time Scales for Gas-Particle
766 Partitioning Equilibration of Secondary Organic Aerosol Formed from Alpha-Pinene
767 Ozonolysis, Environmental Science & Technology, 47, 5588-5594, 10.1021/es400078d,
768 2013.

769 Seinfeld, J. H., and Pandis, S. N.: Atmospheric chemistry and physics : from air pollution
770 to climate change, Third edition. ed., John Wiley & Sons, Inc., Hoboken, New Jersey,
771 xxvi, 1120 pages pp., 2016.

772   Shiraiwa, M., and Seinfeld, J. H.: Equilibration timescale of atmospheric secondary
773   organic aerosol partitioning, Geophys. Res. Lett., 39, 6, 10.1029/2012gl054008, 2012.

774   Tsigaridis, K., Daskalakis, N., Kanakidou, M., Adams, P. J., Artaxo, P., Bahadur, R.,
775   Balkanski, Y., Bauer, S. E., Bellouin, N., Benedetti, A., Bergman, T., Berntsen, T. K.,
776   Beukes, J. P., Bian, H., Carslaw, K. S., Chin, M., Curci, G., Diehl, T., Easter, R. C.,
777   Ghan, S. J., Gong, S. L., Hodzic, A., Hoyle, C. R., Iversen, T., Jathar, S., Jimenez, J. L.,
778   Kaiser, J. W., Kirkevåg, A., Koch, D., Kokkola, H., Lee, Y. H., Lin, G., Liu, X., Luo, G.,
779   Ma, X., Mann, G. W., Mihalopoulos, N., Morcrette, J. J., Müller, J. F., Myhre, G.,
780   Myriokefalitakis, S., Ng, N. L., O'Donnell, D., Penner, J. E., Pozzoli, L., Pringle, K. J.,
781   Russell, L. M., Schulz, M., Sciare, J., Seland, Ø., Shindell, D. T., Sillman, S., Skeie, R.
782   B., Spracklen, D., Stavrakou, T., Steenrod, S. D., Takemura, T., Tiitta, P., Tilmes, S.,
783   Tost, H., van Noije, T., van Zyl, P. G., von Salzen, K., Yu, F., Wang, Z., Wang, Z.,
784   Zaveri, R. A., Zhang, H., Zhang, K., Zhang, Q., and Zhang, X.: The AeroCom evaluation
785   and intercomparison of organic aerosol in global models, Atmos. Chem. Phys., 14,
786   10845-10895, 10.5194/acp-14-10845-2014, 2014.

787   Weitkamp, E. A., Sage, A. M., Pierce, J. R., Donahue, N. M., and Robinson, A. L.:
788   Organic aerosol formation from photochemical oxidation of diesel exhaust in a smog
789   chamber, Environmental Science & Technology, 41, 6969-6975, 10.1021/es070193r,
790   2007.

791   Ye, P., Ding, X., Hakala, J., Hofbauer, V., Robinson, E. S., and Donahue, N. M.: Vapor
792   wall loss of semi-volatile organic compounds in a Teflon chamber, Aerosol Science and
793   Technology, 50, 822-834, 10.1080/02786826.2016.1195905, 2016.

794   Yeh, G. K., and Ziemann, P. J.: Alkyl Nitrate Formation from the Reactions of C-8-C-14
795   n-Alkanes with OH Radicals in the Presence of NOx: Measured Yields with Essential
796   Corrections for Gas-Wall Partitioning, J. Phys. Chem. A, 118, 8147-8157,
797   10.1021/jp500631v, 2014.

798   Yeh, G. K., and Ziemann, P. J.: Gas-Wall Partitioning of Oxygenated Organic
799   Compounds: Measurements, Structure-Activity Relationships, and Correlation with Gas

800 Chromatographic Retention Factor, Aerosol Science and Technology, 49, 726-737,
801 10.1080/02786826.2015.1068427, 2015.

802 Zhang, X., Pandis, S. N., and Seinfeld, J. H.: Diffusion-Limited Versus Quasi-
803 Equilibrium Aerosol Growth, Aerosol Science and Technology, 46, 874-885,
804 10.1080/02786826.2012.679344, 2012.

805 Zhang, X., Cappa, C. D., Jathar, S. H., McVay, R. C., Ensberg, J. J., Kleeman, M. J., and
806 Seinfeld, J. H.: Influence of vapor wall loss in laboratory chambers on yields of
807 secondary organic aerosol, Proc. Natl. Acad. Sci. U. S. A., 111, 5802-5807,
808 10.1073/pnas.1404727111, 2014.

809 Zhang, X., Schwantes, R. H., McVay, R. C., Lignell, H., Coggon, M. M., Flagan, R. C.,
810 and Seinfeld, J. H.: Vapor wall deposition in Teflon chambers, Atmospheric Chemistry
811 and Physics, 15, 4197-4214, 10.5194/acp-15-4197-2015, 2015.
812

813

814

815

816

817

818

819

820

821

822

823

824 **Table 1:** Experimental conditions and results

Expt	Experimental Conditions	Initial Seed aerosol Surface area (μm^2 cm^{-3})	Initial [α-pinene][a] (μg m^{-3})	ΔM_o[b,c] (μg m^{-3})	SOA Mass Yield[d] (%)
1	0.015 M AS, seed only[e]	1090	-	-	-
2	0.05 M AS, seed only[e]	1190	-	-	-
3	0.015 M & 0.05 M AS, seed only[e]	1470	-	-	-
4	0.015 M & 0.05 M AS, seed only[e]	1210	-	-	-
5	0.05 M AS, seed only[f]	8000	-	-	-
6	0.015 M & 0.05 M AS, seed only[f]	8580	-	-	-
7	0.015 M AS, O_3+α-pinene[g,i]	1090	281.8±14.9	71.5±0.5	25.4±1.3
8	0.05 M AS, O_3+α-pinene[g,j]	1260	278.5±13.9	65.9±0.9	23.7±1.2
9	0.05 M AS, O_3+α-pinene[h,k]	9160	283.8±14.2	74.2±1.9	26.1±1.5
10	0.05 M AS, O_3+α-pinene[h,k]	8390	265.8±13.3	71.0±3.4	26.7±1.9
11	0.015 M & 0.05 M AS, O_3+α-pinene[h,l]	8180	289.8±14.5	60.5±1.7	20.9±1.2
12	0.015 M & 0.05 M AS, O_3+α-pinene[h,l]	9440	271.8±13.6	53.7±2.9	19.7±1.4

825 [a]All the α-pinene reacted in the 500 ppb O_3 experiments.

826 [b]The SOA mass concentration (ΔM_o) is calculated using the density = 1.37 g cm^{-3}

827 obtained from the 500 ppb O_3 nucleation experiment in Nah et al. (2016).

828 [c]Uncertainties in the peak SOA mass concentration are calculated from one standard

829 deviation of the aerosol volume as measured by the scanning mobility particle sizer.

830 [d]SOA mass yields at peak SOA growth are reported.

831 [e]Referred to as a "low-SA-seed-only experiment" in the main text.

832 [f]Referred to as a "high-SA-seed-only experiment" in the main text.

833 [g]Referred to as a "low-SA experiment" in the main text.

834 [h]Referred to as a "high-SA experiment" in the main text.

835 [i]Size-dependent particle wall-deposition coefficients obtained from Expt 1 were used for

836 particle wall-deposition correction.

837 [j]Size-dependent particle wall-deposition coefficients obtained from Expt 2 were used for

838 particle wall-deposition correction.

839 [k]Size-dependent particle wall-deposition coefficients obtained from Expt 5 were used for

840 particle wall-deposition correction.

841 [l]Size-dependent particle wall-deposition coefficients obtained from Expt 6 were used for

842 particle wall-deposition correction.

843
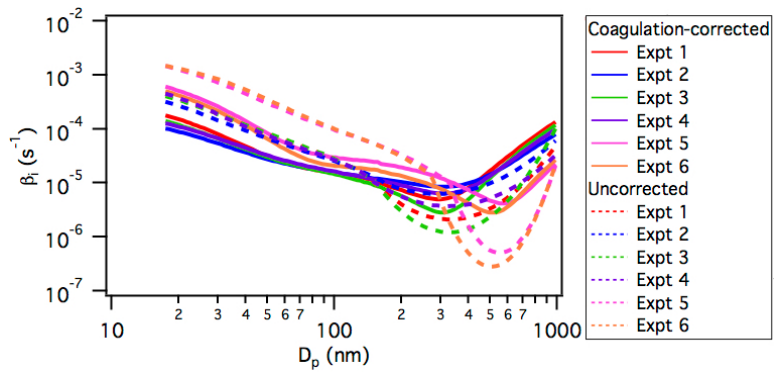
844

845 **Figure 1:** Uncorrected (dashed lines) and coagulation-corrected (solid lines) particle
846 wall-deposition coefficients (β_i) for the low-SA-seed-only (experiments 1 through 4) and
847 high-SA-seed-only (experiments 5 and 6) experiments. Refer to Table 1 for information
848 on the AS solution(s) used to generate the seed aerosol and the initial seed aerosol surface
849 area concentrations in these experiments.

850

851

852

853

854

855
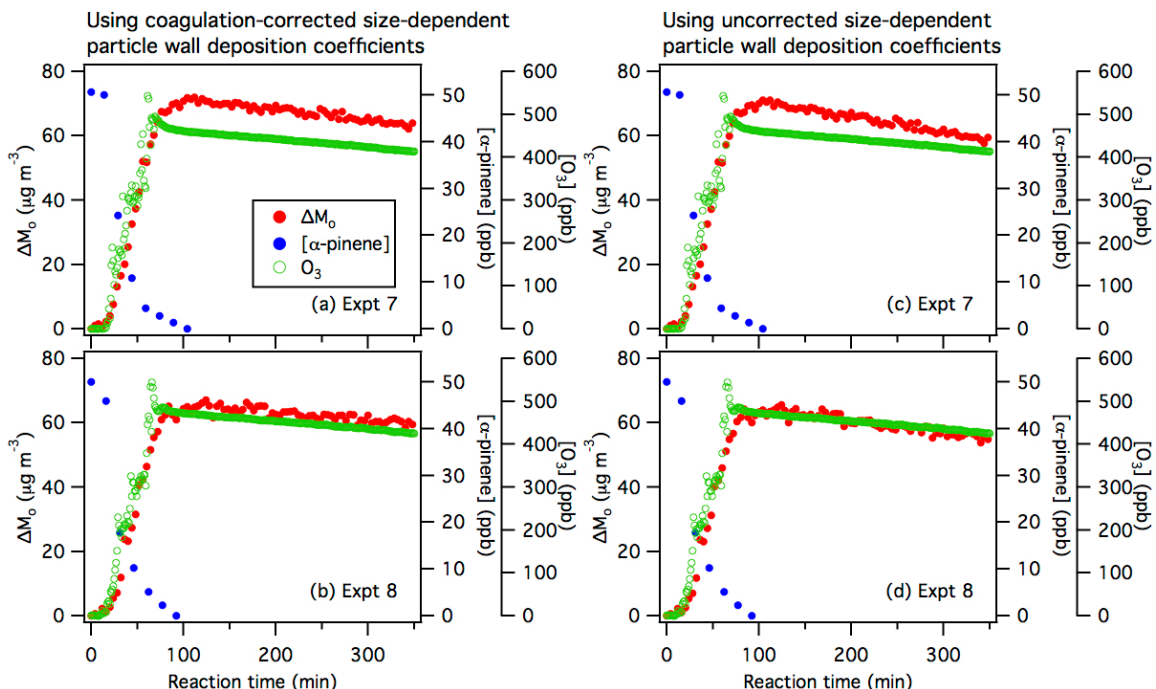
856
857 **Figure 2:** Reaction profiles of the low-SA α-pinene ozonolysis experiments. Panels (a)
858 and (b) show SOA mass concentrations (ΔM_o) obtained using the coagulation-corrected
859 size-dependent particle wall-deposition coefficients from the low-SA-seed-only
860 experiments, while panels (c) and (d) show SOA mass concentrations (ΔM_o) obtained
861 using the uncorrected size-dependent particle wall-deposition coefficients from the low-
862 SA-seed-only experiments. Refer to Table 1 for information on the AS solution(s) used to
863 generate the seed aerosol and the initial seed aerosol surface area concentrations in these
864 experiments.

Figure 3: Reaction profiles of the high-SA α-pinene ozonolysis experiments. Panels (a), (b), (c) and (d) show SOA mass concentrations (ΔM_o) obtained using the coagulation-corrected size-dependent particle wall-deposition coefficients from the high-SA-seed-only experiments, while panels (e), (f), (g) and (h) show SOA mass concentrations (ΔM_o) obtained using the uncorrected size-dependent particle wall-deposition coefficients from the high-SA-seed-only experiments. Refer to Table 1 for information on the AS solution(s) used to generate the seed aerosol and the initial seed aerosol surface area concentrations in these experiments. As explained in the main text, SOA mass concentrations are substantially overestimated when the uncorrected size-dependent particle wall-deposition coefficients are used to account for particle wall deposition.

876
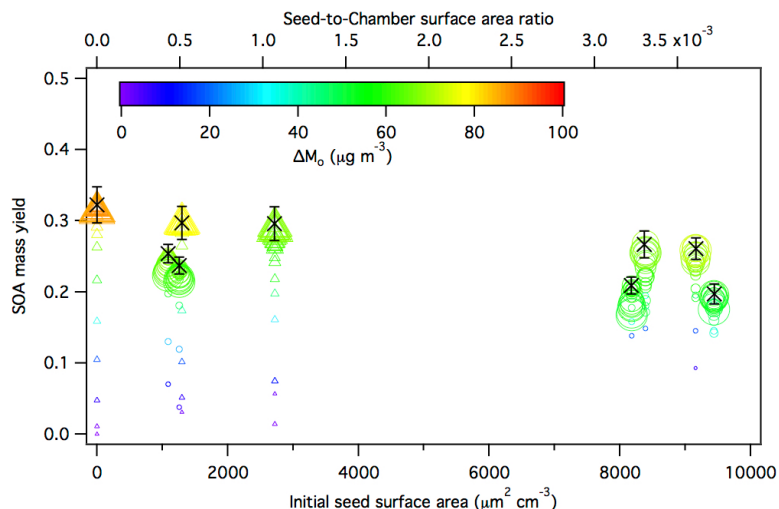
Figure 4: Averaged SOA mass yields over the course of an α-pinene ozonolysis
experiment as a function of initial total AS seed aerosol surface area concentration.
Results from this study (15 min-averaged) are shown as circles, while results from the
study by Nah et al. (2016) (10 min-averaged) are shown as triangles. All the SOA mass
yields shown here (including results from Nah et al. (2016)) are obtained using the
coagulation-corrected size-dependent particle wall-deposition coefficients. Symbol color
indicates the SOA mass concentration and symbol size indicates the time after O_3 is
injected into the chamber. The $\times$ symbols are the SOA mass yields at peak SOA growth
obtained from the experimental data. The y-axis error bars represent the uncertainty in the
SOA mass yield at peak SOA growth, which originates from the α-pinene injection and
the aerosol mass concentration at peak SOA growth (one standard deviation).
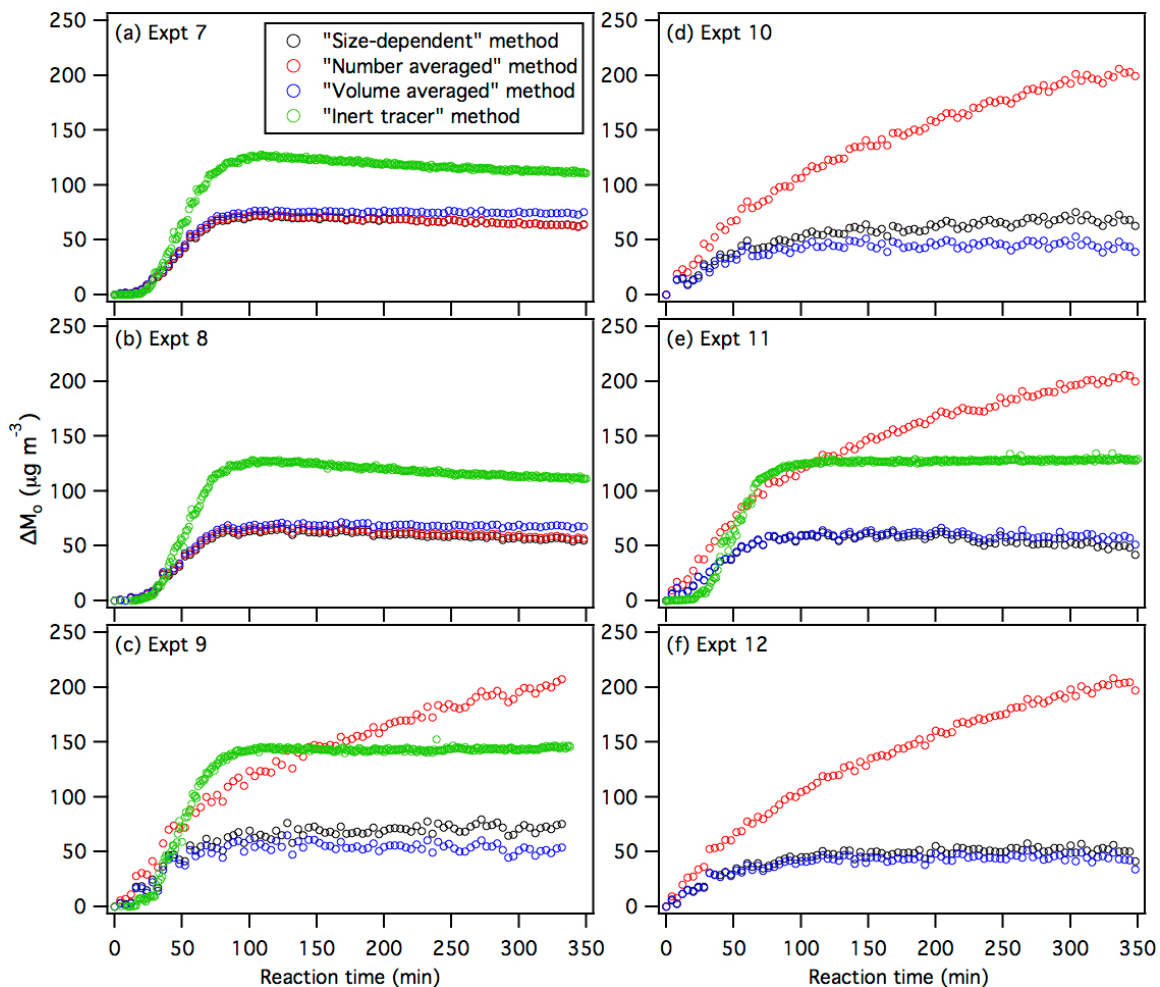
888
889 **Figure 5:** SOA mass concentration (ΔM_o) as a function of reaction time in the α-pinene
890 ozonolysis experiments using the "size-dependent", "number averaged", "volume
891 averaged" and "inert tracer" particle wall-deposition correction methods. HR-ToF-AMS
892 data were not available in experiments 10 and 12, therefore SOA mass concentrations
893 calculated using the "inert tracer" method were not available in these experiments.

894
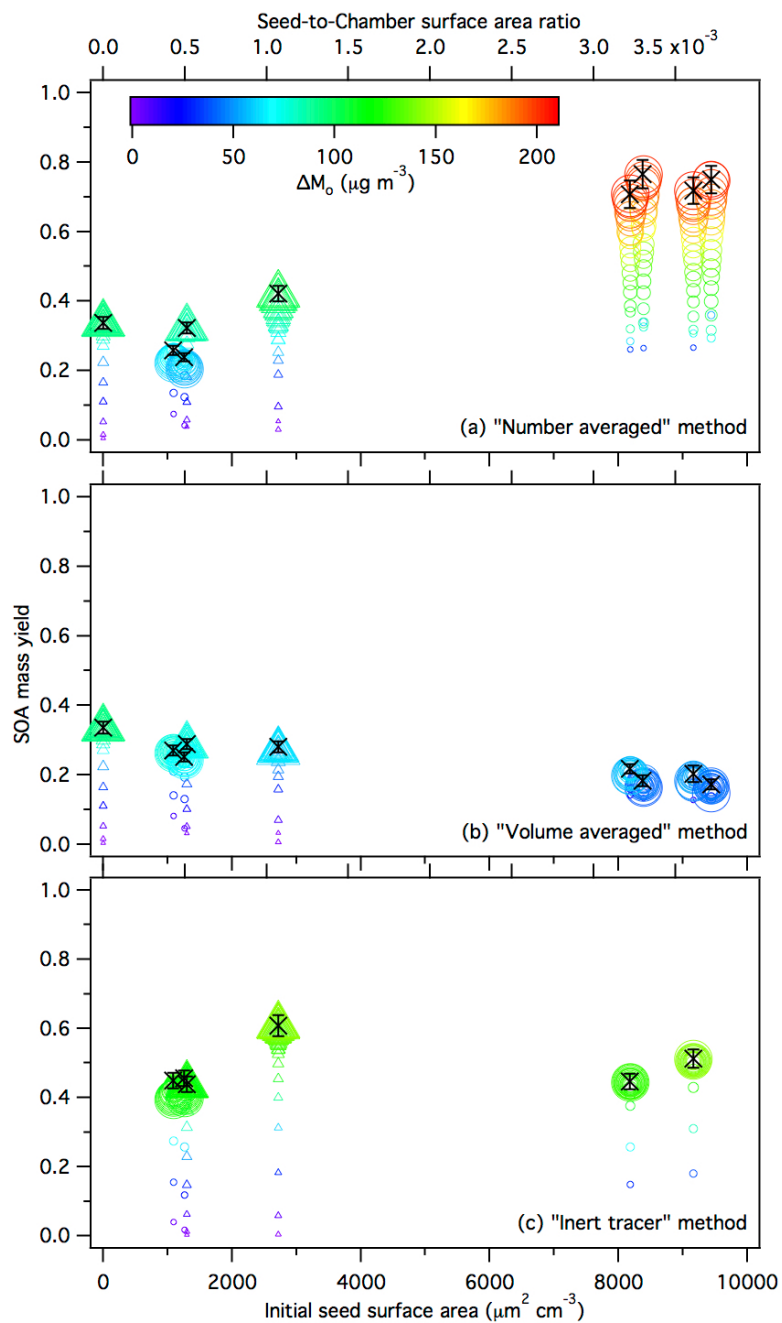
Figure 6: Averaged SOA mass yields over the course of an α-pinene ozonolysis
experiment as a function of initial total AS seed aerosol surface area concentration using
the (a) "number averaged", (b) "volume averaged" and (c) "inert tracer" particle wall-
deposition correction methods. Results from this study (15 min-averaged) are shown as
circles, while results from the study by Nah et al. (2016) (10 min-averaged) are shown as
triangles. Symbol color indicates the SOA mass concentration and symbol size indicates
the time after O_3 is injected into the chamber. The $\times$ symbols are the SOA mass yields at
peak SOA growth obtained from the experimental data. The y-axis error bars represent
the uncertainty in the SOA mass yield at peak SOA growth, which originates from the α-

904 pinene injection and the aerosol mass concentration at peak SOA growth (one standard
905 deviation).